Journal of Nanosciences: Current Research

Bhagat et al., J Nanosci Curr Res 2018, 3:2
DOI: 10.4172/2572-0813.1000122

Research Article Open Access

Effect of Tin and Strontium Doping on the Photocatalytic Activity of Zinc Sulphide Nanoparticles for the Photocatalytic Degradation of Resorcinol under Solar and Ultra-Violet Light

Bhagat MM*, Lokhande P and Mujawar HA

Department of Chemistry, Dr. Babasaheb Ambedkar Technological University, Lonere, Raigad, Maharashtra, India

***Corresponding author:** Madhuri M Bhagat, Department of Chemistry, Dr. Babasaheb Ambedkar Technological University, Lonere, Raigad, Maharashtra, India, Tel: +91 9975636701; E-mail: madhurisd16@gmail.com

Received date: February 3, 2018; **Accepted date:** May 18, 2018; **Published date:** May 25, 2018

Abstract

Tin (Sn) and Strontium (Sr) doped Zinc Sulphide and pure Zinc Sulphide photocatalyst have been prepared by Sol-Gel method. The prepared photocatalyst have been characterised by Thermo gravimetric Differential Thermal Analysis, Scanning Electron Microscopy, Energy Dispersive X-ray, X-Ray Diffraction, ultra-violet visible spectroscopy and photoluminescence spectroscopy. Characterization Techniques have provided information of wurtzite hexagonal structure of Zinc Sulphide. The PL spectra have shown the blue shift of Zinc Sulphide after doping it with Tin and Strontium. Photocatalytic degradation study was done by the complete degradation of an organic pollutant Resorcinol in Sun light as well as in UV-light. The factors affecting the photocatalytic activity of photocatalyst *viz.* pH, catalyst loading and reuse of photocatalyst have been studied along with the photocatalytic degradation of Resorcinol. These external parameters have considerable influenced on the phtocatalytic activity of Zinc Sulphide.

Keywords: Doping; Photocatalyst; Photoluminescence; Pollution; Sol-gel synthesis; Zinc sulphide nanoparticles

Introduction

Resorcinol is one of the pollutants in the effluent of chemical, fertilizer and dye industries and is a typical constituent of coal conversion wastewater. It is released into the environment during production and processing that can cause environmental pollution. It will also be released directly during uses and disposal of resorcinol containing consumer and professional products like hair dye. It is the main content of hair dyes and all non-reacted Resorcinol is rinsed off to the wastewater after the 30-min period of typical use [1].

Resorcinol has many adverse effects on the body of human being. It may cause skin irritation on contact with skin. Inhalation may affect lung or trachea damage and allergic reaction in respiratory track [1]. Also it is listed as an endocrine disruptor [2].

Typical waste water treatments cannot remove the resorcinol and other phenolic compounds completely. Advance Oxidation Process such as (1) O_3/H_2O_2 (2) O_3/Fe^{2+} (3) $UV/O_3/H_2O_2$ (4) O_3 /H_2O_2 /Fe^{2+} have been extensively used. Also the H_2O_2/UV, Fe^{2+}/H_2O_2/UV and TiO_2/UV, TiO_2/H_2O_2/UV photocatalytic processes have been used for the same purpose [3]. But it has more requirements of capital intensive and have some limitations.

In recent years, a cost effective new trend is developed for the complete removal of organic pollutants called photocatalysis. The photocatalysis involves use of semiconductor catalyst which is being active in presence of light for the production of OH radicals. When light of energy greater than band gap energy fall on the surface of the photocatalyst, there occurs formation of electron (e^-) and hole (h^+). The hole has extensive reduction potential that produces OH radicals [4]. The produced OH radicals have highest oxidation potential that can degrade whole organic compound to Carbon dioxide and water [5,6]. Most extensively used semiconductors are TiO_2, ZnO, CdS, WO_3, ZnS and SnO_2 [7].

Amongst the above mentioned photocatalyst Zinc Suphide (ZnS) is an important II-VI wide band-gap semiconductor having excellent physical properties, like size-dependent electrical and optical properties, due to the quantum confinement [8]. It exists in two main crystalline forms. One is the cubic zinc blende (sphalerite) and the other is the hexagonal wurtzite. Both are crystalline forms having band gaps of 3.54 eV and 3.77 eV belong to cubic zinc blende and hexagonal wurtzite ZnS respectively [4]. Cubic Zinc blende structure of Zinc Sulphide is more stable than the hexagonal structure. Very few work was noticed in the field of photocatalytic activity of metal co-doped Zinc Sulphide. Earliar researchers have studied the effect of metal and non metal doping on the Zinc Sulphide nanoparticles thereby successful decrease in band gap but shows 50-80% degradation efficiency [7]. In this attempt co-doping of the metals have been studied with doping of Tin and Strontium. The incorporation of Sn and Sr decreases the band gap and increases the photocatalytic activity of Zinc Sulphide with complete degradation of resorcinol.

Photocatalytic semiconducting materials have been prepared by various methods like Chemical co-precipitation, Chemical bath deposition, Hydrothermal, Sol-Gel, microwave, Successive Ionic Layer Adsorption and Reaction, Mechano-chemical method etc. [8-11]. In present study Zinc Sulphide nanoparticles were prepared by Sol-Gel method. It involves conversion of monomers into a colloidal solution i.e., sol which on heating converts to gel (an integrated network). Gel on calcination forms fine nanosized particles. This is very effective and widely used method for semiconductor synthesis.

Materials and Methods

Chemicals used for the preparation of Zinc Sulphide nanoparticles were of analytical grade reagents. It were used without further purification. For the preparation of Pure Zinc Sulphide, Zinc Acetate dihydrate Zn $(CH_3COO)_2.2H_2O$ and Thiourea $(CS(NH_2)_2)$ were taken in a molar proportion (0.1 M). For the doping of metals Strontium and Tin, Strontium Nitrate Sr $(NO_3)_2$ and Stannous Chloride SnCl2.2H2O were taken respectively. Four samples of different proportions A-($Sn_{0.02}$, $Sr_{0.08}$: ZnS), B-($Sn_{0.04}$, $Sr_{0.06}$: ZnS), C-($Sn_{0.06}$, $Sr_{0.04}$: ZnS) and D-($Sn_{0.08}$, $Sr_{0.02}$: ZnS) were prepared. These samples were prepared by applying the molar proportion formula Snx Sry $Zn_{x(1-x+y)}$S.

For the preparation of doped Zinc Sulphide, appropriate weights of required chemicals were dissolved in 100 ml methanol. Firstly Solutions of Zinc Acetate, Strontium Nitrate and Stannous Chloride were mixed and stirred on the magnetic stirrer for 10 minutes. Then Thiourea solution was added drop wise for proper nucleation. 25 ml ethylene glycol was also added as a capping agent. The temperature was raised to 80°C. This mixture was continuously stirred for 6 hours. Initially colourless sol is formed which was then turned to pink colour gel. This gel was dried on magnetic stirrer and calcined at 750°C in muffle Furnace for an hour. After Calcination product were collected and taken for characterisation. Same procedure was repeated for the synthesis of pure zinc sulphide by using Zinc Acetate and Thiourea.

The samples were characterised by TG-DTA, XRD, SEM-EDX and UV-Visible spectroscopy. Photocatalytic activity of the doped and undoped photocatalyst were studied by degrading 100 ml of 20 ppm Resorcinol solution in visible light as well as in UV light.

Results and Discussion

Characterisation

In the Characterisation of samples, Morphology was studied by Scanning Electron Microscopy (SEM), Crystal structure by X-Ray Diffraction (XRD), Calcination temperature Thermal Gravimetric Differential Thermal Analysis (TG-DTA), Optical Study by UV-Visible Spectroscopy and photoluminescence Spectroscopy.

TGA analysis

Thermal properties of ZnS prepared by Sol-Gel method were studied with the TG-DTA. The TGA-DTA graph for prepared Zinc Sulphide nanoparticles is shown in Figure 1.

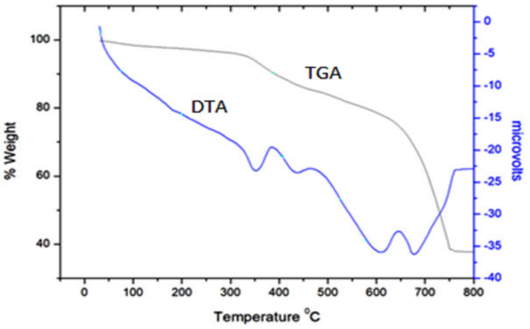

Figure 1: TGA-DTA graph for prepared zinc sulphide nanoparticles.

The thermal stability of the nanocomposites was found at 750°C. Up to this temperature structural changes take place. No change in weight of ZnS was found after 750°C. So the all samples of doped Zinc Sulphide were calcined on 750°C temperature.

Scanning electron microscopy (SEM)

Morphological study of pure and Sr and Sn doped Zinc Sulphide prepared by Sol-Gel method was carried out by Scanning Electron Microscopy. Figure 2 shows the SEM images for A-($Sn_{0.02}$, $Sr_{0.08}$: ZnS), B-($Sn0_{.04}$, $Sr_{0.06}$: ZnS), C-($Sn_{0.06}$, $Sr_{0.04}$: ZnS), D-($Sn_{0.08}$, $Sr_{0.02}$: ZnS) and E-Pure ZnS respectively.

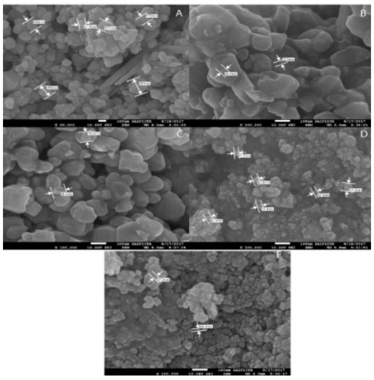

Figure 2: SEM images of A-($Sn_{0.02}$, $Sr_{0.08}$: ZnS), B-($Sn_{0.04}$, $Sr_{0.06}$: ZnS), C-($Sn_{0.06}$, $Sr_{0.04}$: ZnS), D-($Sn_{0.08}$, $Sr_{0.02}$: ZnS) and E-Pure ZnS respectively.

The SEM images for each sample gives the idea of the spherical shape crystals of pure and Sr and Sn doped zinc sulphide. Crystals appears mostly hexagonal shape which was further confirmed by XRD.

Energy dispersive X-ray spectroscopy (EDX)

Elemental analysis of prepared pure and doped Zinc Sulphide executed by Energy Dispersive X-Ray Speectroscopy. Figure 3 shows the EDX images of ($Sn_{0.02}$, $Sr_{0.08}$: ZnS), ($Sn_{0.04}$, $Sr_{0.06}$: ZnS), ($Sn_{0.06}$, $Sr_{0.04}$: ZnS), ($Sn_{0.08}$, $Sr_{0.02}$: ZnS) and Pure ZnS respectively.

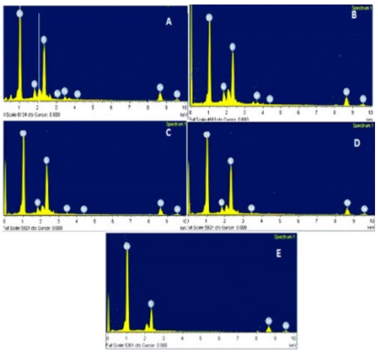

Figure 3: EDX images of A-($Sn_{0.02}$, $Sr_{0.08}$: ZnS), B-($Sn_{0.04}$, $Sr_{0.06}$: ZnS), C-($Sn_{0.06}$, $Sr_{0.04}$: ZnS), D-($Sn_{0.08}$, $Sr_{0.02}$: ZnS) and E-Pure ZnS respectively.

The EDX images 3A, 3B, 3C and 3D shows the presence of Sr and Sn peaks indicating the successful assimilation of these elements in the crystal of Zinc Sulphide. Image 5E is the EDX image of pure Zinc sulphide showing the abundant peak for Zinc and Sulphur. The above EDX images reveal the successful doping of Tin and Strontium in the crystals lattice of Zinc sulphide.

X-ray diffraction analysis (XRD)

Crystal structure of the pure and doped Zinc Sulphide was confirmed by means of planes of Zinc Sulphide determined by the XRD analysis. Particle size of prepared Zinc Sulphide by Sol-Gel method was calculated from XRD data. Figure 4 is the XRD ghraph for Samples A, B, C, D and E respectively.

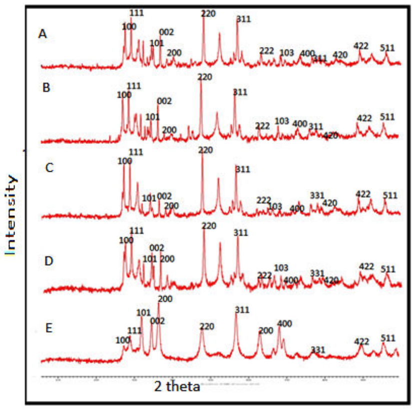

Figure 4: XRD graph for A-($Sn_{0.02}$, $Sr_{0.08}$: ZnS), B-($Sn_{0.04}$, $Sr_{0.06}$: ZnS), C-($Sn_{0.06}$, $Sr_{0.04}$: ZnS), D-($Sn_{0.08}$, $Sr_{0.02}$: ZnS) and E-Pure ZnS respectively.

The XRD planes present in graph E *viz.* 100, 111, 101, 002, 200, 220, 311, 400, 331, 422 and 511 are the planes that belongs to 2θ values 27.19°, 28.84°, 31.87°, 34.41°, 36.39°, 52.09°, 56.67°, 62.97°, 69.13°, 77°, 95.17° respectively representing the Wurtzite (Hexagonal) structure of Zinc Sulphide which are perfectly matches with JCPDS Card No. 39-1363. Beside this, graph A, B, C, D shows additional planes 103, 420, 222 which are present because of Sr and Sn doping. 420 is for Sn and 103 and 222 are the planes for Sr impurity.

The particle size of pure and Sr and Sn doped Zinc Sulphide was calculated for each sample of Zinc Sulphide by using Sherrer Equation:

$d = n\lambda/\beta\cos\theta$

For the Sn and Sr doped samples A, B, C and D 220 plane has chosen for the calculation of particle size because it have relative intensity 100%, belonging to 2θ values 47.71°, 47.64°, 47.69°, 47.70° respectively. Plane 200 is used for pure Zinc Sulphide corresponded to 36.39°.

Particle size of each sample of Zinc sulphide (doped and undoped) is listed as in Table 1.

S.No	Sample	Particle Size nm
1	$Sn_{0.02}$, $Sr_{0.08}$: ZnS	90.2
2	$Sn_{0.04}$, $Sr_{0.06}$: ZnS	135
3	$Sn_{0.06}$, $Sr_{0.04}$: ZnS	90.35
4	$Sn_{0.08}$, $Sr_{0.02}$: ZnS	77.3
5	Pure ZnS	135.6

Table 1: Particle size for for A-($Sn_{0.02}$, $Sr_{0.08}$: ZnS), B-($Sn_{0.04}$, $Sr_{0.06}$: ZnS), C-($Sn_{0.06}$, $Sr_{0.04}$: ZnS), D-($Sn_{0.08}$, $Sr_{0.02}$: ZnS) and E-Pure ZnS.

From the Table 1 Sample D $Sn_{0.08}$, $Sr_{0.02}$: ZnS have smallest particle size 77.3 nm amongst the rest of the Sr and Sn doped and pure Zinc Sulphide samples prepared by Sol-Gel method.

B-$Sn_{0.04}$, $Sr_{0.06}$: ZnS and pure Zinc Sulphide have the particle size 135 nm that may show the lowest photocatalytic activity than the other samples. The prepared photocatalysts A $Sn_{0.02}$, $Sr_{0.08}$: ZnS and C-$Sn_{0.06}$, $Sr_{0.04}$: ZnS have the particle size 90.2 nm and 90.35 nm respectively calculated by Sherrer formula.

UV-Visible spectroscopy

UV-Visible spectroscopic analysis is used for the calculation of band gap by measuring wavelength maximum for each sample. The wavelength maximum of prepared pure and doped zinc sulphide was checked on the Equiptronics EQ 820 UV-Visible spectrophotometer. From the λmax data, band gap was calculated by using the formula,

Band Gap Energy (E) = h*C/λ

Where,

h = Planks constant

C = Speed of light

λ = Cut off wavelength

The Figure 5 is showing the UV-Visible spectra of doped and undoped Zinc Sulphide nanoparticles. Band gap energies for Sn and Sn doped Zinc Sulphide and Pure Zinc Sulphide are given in Table 2.

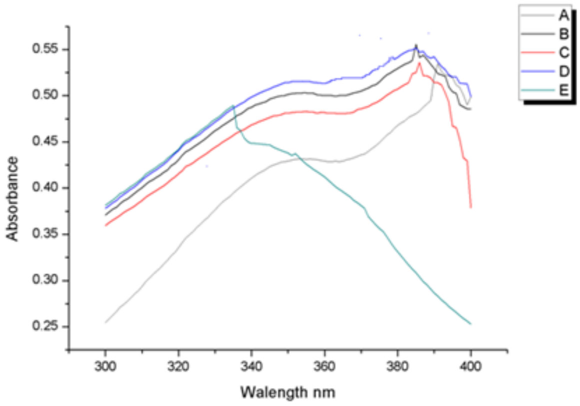

Figure 5: UV-Visible spectra for A-($Sn_{0.02}$, $Sr_{0.08}$: ZnS), B-($Sn_{0.04}$, $Sr_{0.06}$: ZnS), C-($Sn_{0.06}$, $Sr_{0.04}$: ZnS) , D-($Sn_{0.08}$, $Sr_{0.02}$: ZnS) and E-Pure ZnS respectively.

S.No	Samples	Wavelengh λmax	Band Gap eV
1	$Sn_{0.02}Sr_{0.08}ZnS$	391 nm	3.1
2	$Sn_{0.04}Sr_{0.06}ZnS$	385 nm	3.22

3	$Sn_{0.06}Sr_{0.04}ZnS$	386 nm	3.21
4	$Sn_{0.08}Sr_{0.02}ZnS$	385 nm	3.22
5	Pure ZnS	335 nm	3.7

Table 2: Band gap energies of strontium and tin doped and undoped zinc sulphide nanoparticles.

Band gap of Pure Zinc Sulphide prepared by Sol-Gel method was found to 3.70 eV that exactly the band gap of hexagonal Zinc Sulphide. This band was then decreased for all the samples. For sample it was 3.1 eV as there was higher concentration of Strontium and it remained almost constant for sample B, C and D. It was found to be 3.2 eV.

Photoluminescence spectroscopy

The photoluminescence spectra of all the five samples with the excitation wavelength of 300 nm shows the emission peak for Sn and Sr doped zinc sulphide and pure Zinc sulphide as shown in Figure 6.

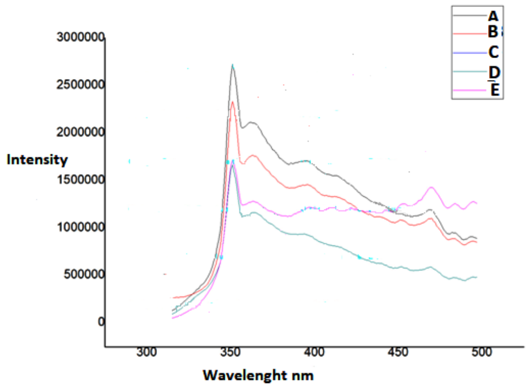

Figure 6: Photoluminescence spectra for A-($Sn_{0.02}$, $Sr_{0.08}$: ZnS), B-($Sn_{0.04}$, $Sr_{0.06}$: ZnS), C- ($Sn_{0.06}$, $Sr_{0.04}$: ZnS), D-($Sn_{0.08}$, $Sr_{0.02}$: ZnS) and E-Pure ZnS respectively.

The pure Zinc Sulphide prepared by Sol-Gel method (E) has shown broad emission peak at 469 nm which was shifted to the shorter wavelength on doping with Tin and Strontium. For sample A ($Sn_{0.02}$, $Sr_{0.08}$: ZnS) it was at 363nm and for B-($Sn0_{.04}$, $Sr_{0.06}$: ZnS) it was located at 353 nm. While for photocatalysts C-($Sn_{0.06}$, $Sr_{0.04}$: ZnS) and D-($Sn_{0.08}$, $Sr_{0.02}$: ZnS) the emission peak was at 350 nm. In summary on doping with the Tin and Strontium to the Zinc Sulphide the emission band shifted towards the blue shift. This blue shift of ZnS on doping with the Sn and Sr is due to the higher crystallinity of doped ZnS than the pure ZnS [12-14].

Photocatalytic degradation experiments

Photocatalytic reaction experiments were carried out in solar light and in an UV light. For both light source reaction, the 100 ml of resorcinol solution was loaded with 100 mg of pure and Sr and Sn doped zinc sulphide photocatalyst.

Photocatalytic degradation experiment in UV light

For the UV light photocatalytic degradation experiment, special UV-light chamber called UV-photoreactor was used. In the reaction vessel of UV photoreactor 100 ml of 20 ppm Resorcinol solution was stirred with 100 mg of photocatalyst. The temperature of the reaction vessel was maintained below 25°C to avoid decomposition of Resorcinol by thermal decomposition. The light source used was 13 watt UV lamp that produces 4210 lux intense light which was measured by lux meter. Photocatalytic degradation reaction experiments were executed for each sample of Sr and Sn doped Zinc Sulphide and pure Zinc Sulphide for about 90 minutes. The samples were collected for the determination of COD at 15 minutes time interval.

The calculated COD of 20 ppm Resorcinol was found to be 320 ppm. From Table 3 it is observed that pure Zinc Sulphide prepared by sol-gel method Showed 90% degradation of Resorcinol. But the sample A $Sn_{0.02}Sr_{0.08}ZnS$, C $Sn_{0.06}Sr_{0.04}ZnS$ and D $Sn_{0.08}Sr_{0.02}ZnS$ showed the complete degradation of Resorcinol. Among these three catalysts, D $Sn_{0.08}Sr_{0.02}ZnS$ catalyst is the fastest catalyst for the degradation of Resorcinol. This is because the particle size of these catalysts is smaller than pure Zinc Sulphide that provided large surface area for the photocatalytic reaction.

Time in minutes	COD for Pure ZnS	COD for $Sn_{0.02}Sr_{0.08}ZnS$	COD for $Sn_{0.04}Sr_{0.06}ZnS$	COD for $Sn_{0.06}Sr_{0.04}ZnS$	COD for $Sn_{0.08}Sr_{0.02}ZnS$
15	88	120	88	160	80
30	72	96	80	144	40
45	56	48	80	24	8
60	56	32	40	24	0
75	32	0	40	0	0
90	32	0	40	0	0

Table 3: COD for A-($Sn_{0.02}$, $Sr_{0.08}$: ZnS), B-($Sn_{0.04}$, $Sr_{0.06}$: ZnS), C-($Sn0_{.06}$, $Sr_{0.04:}$ ZnS), D- ($Sn_{0.08}$, $Sr_{0.02}$: ZnS) and E-Pure ZnS respectively in UV light.

Citation: Bhagat MM, Lokhande P, Mujawar HA (2018) Effect of Tin and Strontium Doping on the Photocatalytic Activity of Zinc Sulphide Nanoparticles for the Photocatalytic Degradation of Resorcinol under Solar and Ultra-Violet Light. J Nanosci Curr Res 3: 122. doi: 10.4172/2572-0813.1000122

Photocatalytic degradation in solar light

For the solar light Photodegradation by prepared pure and Strontium and Tin doped Zinc Sulphide, 100 ml Resorcinol solution loaded with 100 mg of photocatalyst was stirred for six hours under sun light. The samples were collected at each for the determination COD for each hour. The calculated COD for 20 ppm Resorcinol was 320 ppm as mentioned above.

It was observed from Table 4 that amongst all the photocatalysts prepared by sol-gel method, $Sn_{0.08}Sr_{0.02}ZnS$ shown highest and complete degradation of Resorcinol after six hour Photodegradation. $Sn_{0.08}Sr_{0.02}ZnS$ photocatalyst has lowest particle size 77.3 nm than the rest of the photocatalysts that provides wide surface for the photocatalytic reaction.

Time in hour	COD for Pure ZnS	COD for $Sn_{0.02}Sr_{0.08}ZnS$	COD for $Sn_{0.04}Sr_{0.06}ZnS$	COD for $Sn_{0.06}Sr_{0.04}ZnS$	COD for $Sn_{0.08}Sr_{0.02}ZnS$
1	120	40	120	120	88
2	112	40	104	80	72
3	112	40	80	80	40
4	96	40	65	80	40
5	80	32	40	48	24
6	64	32	40	38	0

Table 4: COD for for A-($Sn_{0.02}$, $Sr_{0.08}$: ZnS), B-($Sn_{0.04}$, $Sr_{0.06}$: ZnS), C-($Sn_{0.06}$, $Sr_{0.04}$: ZnS), D-($Sn_{0.08}$, $Sr_{0.02}$: ZnS) and E-Pure ZnS respectively for solar light photodegradation Resorcinol.

Effect of catalyst loading

Catalyst dosage is extrinsic parameter that directly affects the photocatalytic activity of photocatalyst. The effect of dosage of photocatalyst was studied by loading the each samples i.e., for A-($Sn_{0.02}$, $Sr_{0.08}$: ZnS), B-($Sn_{0.04}$, $Sr_{0.06}$: ZnS), C-($Sn_{0.06}$, $Sr_{0.04}$: ZnS) , D-($Sn_{0.08}$, $Sr_{0.02}$: ZnS) and E-Pure ZnS samples. 50 mg, 100 mg, 150 mg and 200 mg of each photocatalyst sample was mixed with 100 ml of 20 ppm Resorcinol solution and stirred for 6 hours under Solar light. The samples were irradiated with sunlight with constant stirring for about six hours. Figure 7 showing the graphs for effect of catalyst loading for Sample A, B, C, D and E samples for Sn and Sr doped Zinc Sulphide and Pure Zinc Sulphide.

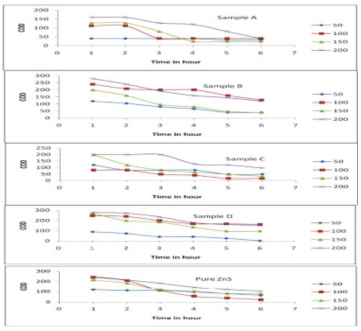

Figure 7: Effect of catalyst loading for A-($Sn_{0.02}$, $Sr_{0.08}$: ZnS), B-($Sn_{0.04}$, $Sr_{0.06}$: ZnS), C- ($Sn_{0.06}$, $Sr_{0.04}$: ZnS), D-($Sn_{0.08}$, $Sr_{0.02}$: ZnS) and E-Pure ZnS respectively.

For all the doped and undoped Zinc Sulphide nanoparticles prepared by sol-gel method 50 mg and 100 mg catalysts shown the highest photocatalytic activity than the rest 150 mg and 200 mg catalyst concentration. As the catalyst concentration increases less light radiation falls on the surface of the photocatalyst because of rush of catalyst particles. Optimum catalysts concentration for the Zinc Sulphide is 50mg/100ml Resorcinol that shown clearly highest degradation rate for A-($Sn_{0.02}$, $Sr_{0.08}$: ZnS), B-($Sn_{0.04}$, $Sr_{0.06}$: ZnS), , D-($Sn_{0.08}$, $Sr_{0.02}$: ZnS) and for C-($Sn0_{.06}$, $Sr_{0.04}$: ZnS) E-Pure ZnS both 100mg and 50 mg shown similar degradation rate.

pH effect

pH is an extrinsic parameter that affects the phtocatalytic activity of the photocatalyst. This study was done by performing the degradation of 20 ppm resorcinol (100 ml) dosed with 50 mg of photocatalyst in presence of UV light. The proportion of catalysts and resorcinol solution was kept same for all doped and undoped zinc sulphide nanoparticles samples. The reaction was carried out for 90 minutes. The samples were taken out for the determination of COD at 15 minutes time interval. The graph of pH effect for samples A, B, C, D and E is illustrated in Figure 8.

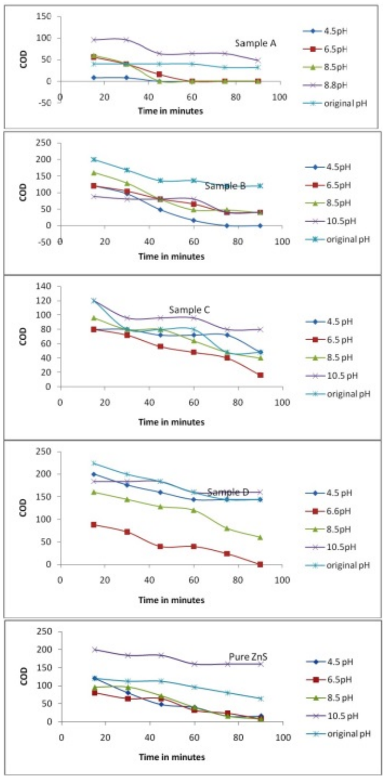

Figure 8: pH effect for A-($Sn_{0.02}$, $Sr_{0.08}$: ZnS), B-($Sn_{0.04}$, $Sr_{0.06}$: ZnS), C-($Sn_{0.06}$, $Sr_{0.04}$: ZnS), D-($Sn_{0.08}$, $Sr_{0.02}$: ZnS) and E-pure ZnS respectively.

The photocatalyst surface is positively charged in acidic solutions and negatively charged in alkaline solutions [15-18]. Since resorcinol is weakly acidic in nature that shows degradation at near about neutral pH.

The actual pH of the resorcinol and catalyst suspension was noted 5.8 pH. At this pH surface of the catalyst have zero point charge [8]. Above this pH surface charge become negatively charged hence more adsorption of resorcinol on the surface of the catalyst promoting the degradation at higher pH than the original one.

The prepared catalysts Sr and Sn doped ZnS and Pure ZnS shows more degradation at pH 6.5. The pH 6.5 is the optimum pH for strontium and tin doped zinc sulphide photocatalyst.

Reutilisation of photocatalyst

Reutilisation of above Sr and Sn doped Zinc Sulphide and pure Zinc Sulphide prepared by Sol-Gel method was checked by collecting the photocatalyst after use. The collected photocatalyst was washed with water several times and completely dried in an oven. These dried catalysts were loaded with 50 mg/50 ml of 20 ppm Resorcinol solution. The photocatalytic reaction was carried out for each catalyst sample for five hours in sunlight. This process was repeated thrice. The initial COD and COD after five hours were determined. It was found that there was no change in the photocatalytic activity of photocatalyst after using twice.

Conclusion

Strontium and Tin doped Zinc Sulphide and pure Zinc sulphide were synthesized by Sol-Gel method. The synthesized photocatalyst have nano sized hexagonal wurtzite structure confirmed by XRD analysis. The band gap of pure Zinc Sulphide (3.7 eV) is lowered by doping it with Sr and Sn (3.2 eV) with enhanced photocatalytic activity. A PL spectrum shows the blue shift of doped Zinc Sulphide. The photocatalytic activity of Sr and Sn doped catalyst is better than pure Zinc Sulphide prepared by Sol-Gel method in UV light. 50 mg/100 ml is the optimum quantity for catalyst loading. Acidic pH favours the fast degradation Resorcinol. Sn and Sn doped Zinc Sulphide photocatalyst can be reused with retaining photocatalytic activity.

Acknowledgement

All the experimental work was supported by Dr. Babasaheb Ambedkar Technological University Lonere Raigad, SAIF, IIT Bombay and IIT Madras, India. This research did not receive any specific grant from funding agencies in the public, commercial, or not-for-profit sectors.

Contribution of Authors

The authors declare that this work was done by the authors named in this article and all liabilities pertaining to claims relating to the content of this article will be borne by them. Madhuri M. Bhagat carried out the research work. Dr.PB Lokhande and Dr.HA Mujawar supervised the whole research work. All authors have reviewed and approved the content of the submitted manuscripts.

Conflict of Interest

No conflict of interest is associated with this work.

References

1. Hahn S (2006) Concise International chemical assessment document. World Health Organization, Geneva.
2. Amaral MJJ (2002) The endocrine disruptors: a major medical challenge. Food Chemical Technology 40: 781-788.
3. Pouran SR, Aziz ARA, Daud WMAW (2014) Review on the advances in photo-Fenton oxidation system for the recalcitrant wastewater. J Ind Eng Chem 21: 53-69.
4. Pardeshi SK, Patil AB (2009) Solar photocatalytic degradation of resorcinol a model endocrine disruptor in water using Zinc Oxide J Hazard Mater 163: 403-409.
5. Pirhashemi M, Habibi-Tangjeh A, Pouran SR (2018) Review on the criteria anticipated for the fabrication of highly efficient ZnO-based visible-light driven photocatalysts. J Ind Eng Chem 62: 1-25.
6. Lawless D, Serpone N, Meisel D (1991) Role of OH radicals and trapped holes in photocatalysis. A Pulse Radlolysls Study. J Phys Chem A 95: 5166-5170.
7. Zegeye DZ, Yadav OP, Mengesha AT (2017) Photocatalytic activity of Mn-N co-doped ZnS nanoparticles for the degradation of organic pollutant (Methylene Blue). IJPSR 1: 39-50.
8. Hamendez-Ramirez A, Medina-Ramirez I (2015) Photocatalytic semiconductors synthesis, characterisation and environmental applications. Springer International Publishing, New York. p. 289.
9. Mukherjee A, Mitra P (2015) Structural and optical characteristics of SnS thin film prepared by SILAR. Mat Sci 33: 847-851.

10. Bhagat MM, Lokhande PB, Mujawar HA (2017) Photocatalytic degradation of carcinogenic rhodamine 6g dye by strontium and tin doped cadmium sulphide nanoparticles. IJRPET 3: 129-136.
11. Xua C, Deb S, Baluc AM, Ojedad DM, Luqued R (2015) Mechanochemical synthesis of advanced nanomaterials for catalytic applications. Chem Comm 31: 16.
12. Jiang D, Cao L, Liu W, Su G, Qu H, et al. (2009) Synthesis and luminescence Properties of Core/Shell ZnS:Mn/ZnO Nanoparticles Nanoscale Res Letter 4: 78-8.
13. Fang, XS (2011) ZnS nanostructures: from synthesis to applications. Prog Mat Sci 56: 175-287.
14. Tolia JV, Chakraborty M, Murthy ZVP (2012) Photocatalytic degradation of malachite green dye using doped and undoped ZnS nanoparticles. Pol J Chem Tech 14: 16-21.
15. Tang WZ, Huang CP (1995) Inhibitory effect of thioacetamide on CdS dissolution during photocatalytic oxidation of 2,4-dichlorophenol. Chemosphere 30: 1385-1399.
16. Wu X, Li K, Wang H (2009) Facile synthesis of ZnS nanostructured spheres and their photocatalytic properties. J Alloys Compd 487: 537-544.
17. Pouran SR, Bayrami A, Raman AAA, Daud WMAW, Shafeeyan MS, et al. (2018) Comprehensive study on the influence of molybdenum substitution on characteristics and catalytic performance of magnetite nanoparticles. Res Chem Intermed 44: 883- 900.
18. Khatae A, Hassandoost R, Pouran SR (2018) Cerium Substituted magnetite: Fabrication, Characterization and sonocatalytic assessment. Ultrason Sonochem 41: 626-640.